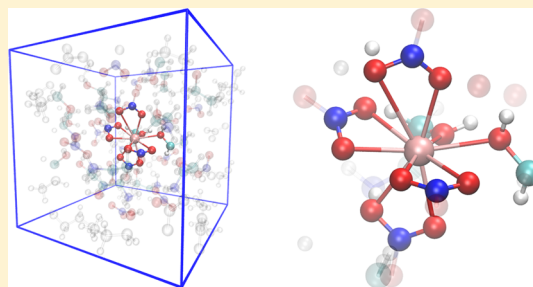


# Lanthanum(III) and Lutetium(III) in Nitrate-Based Ionic Liquids: A Theoretical Study of Their Coordination Shell

Enrico Bodo\*

Department of Chemistry, University of Rome "La Sapienza", P. A. Moro 5, 00185, Rome, Italy

**ABSTRACT:** By using *ab initio* molecular dynamics, we investigate the solvent shell structure of  $\text{La}^{3+}$  and  $\text{Lu}^{3+}$  ions immersed in two ionic liquids, ethylammonium nitrate (EAN) and its hydroxy derivative (2-ethanolammonium nitrate, HOEAN). We provide the first study of the coordination properties of these heavy metal ions in such a highly charged nonaqueous environment. We find, as expected, that the coordination in the liquid is mainly due to nitrate anions and that, due to the bidentate nature of the ligand, the complexation shell of the central ion has a nontrivial geometry and a coordination number in terms of nitrate molecules that apparently violates the decrease of ionic radii along the lanthanides series, since the smaller  $\text{Lu}^{3+}$  ion seems to coordinate six nitrate molecules and the  $\text{La}^{3+}$  ion only five. A closer inspection of the structural features obtained from our calculations shows, instead, that the first shell of oxygen atoms is more compact for  $\text{Lu}^{3+}$  than for  $\text{La}^{3+}$  and that the former coordinates 8 oxygen atoms while the latter 10 in accord with the typical lanthanide's trend along the series and that their first solvation shells have a slight irregular and complex geometrical pattern. When moving to the HOEAN solutions, we have found that the solvation of the central ion is possibly also due to the cation itself through the oxygen atom on the side chain. Also, in this liquid, the coordination numbers in terms of oxygen atoms in both solvents is 10 for  $\text{La}^{3+}$  and 8 for  $\text{Lu}^{3+}$ .



## INTRODUCTION

Solvation is the ubiquitous phenomenon that lie at the basis of the chemical behavior and reaction processes in liquids. The solvation processes control the dissolution and diffusion of ionic and neutral species, and their understanding is crucial for the optimal design of many industrial and extraction processes. The dissolution and the complexation of lanthanoid(III) ions,  $\text{Ln}^{3+}$ ,<sup>1–4</sup> may represent a very effective route for the separation of these elements. It therefore follows that the physical characterization of the structure of their solvation shell is mandatory to select the best performing solvents.<sup>5</sup> The separation of  $\text{Ln}^{3+}$  ions from nuclear waste is currently done by employing organic solvents to extract them from the aqueous phases with different techniques and operating conditions. Among the various substances that can be used in the separation processes, ionic liquids may represent a viable and effective route<sup>6–8</sup> because of their unique solvating abilities<sup>9</sup> and their chemical stability.

Ionic liquids (ILs) are one of the most promising classes of solvents nowadays available and one of the most investigated materials of the last decades.<sup>10–13</sup> The possibility of tuning their physical properties with changes in their chemical structure has motivated the use of these materials as “tunable solvents” for an impressive range of technical applications. The complicated relation between the macroscopic properties of these substances and their nanoscopic structure ultimately depends on the rather entangled interplay between the molecular “shapes” of the constituents and the energetic balance between the long-range electrostatic forces, the short-range van der Waals ones, and possibly hydrogen bonding.

The latter is particularly important in the subset of ILs known as *protic ionic liquids* that can be prepared<sup>14</sup> through an acid–base reaction that leads to the formation of a liquid entirely made of charged species where proton acceptor and donor sites eventually generate a hydrogen-bonded network (e.g., see refs 15–18).

In recent years, the development and the growth of computational power has allowed the theoretical community to provide a rather accurate nanoscopic interpretation of many bulk properties of such complex materials.<sup>16,18,19</sup> One of the possible approaches which have been used to tackle the problem of a microscopic description of ionic liquids is *ab initio* molecular dynamics (AIMD),<sup>16,20–24</sup> even though these simulations are still limited to very short time scales and small spatial dimensions due to the poor performance of AIMs with respect to classical MD.<sup>25</sup>

In this view, we present here a study in which we employ first principle molecular dynamics in order to interpret the structure of the solvation shell of lanthanoid(III) ions immersed in ethylammonium nitrate (EAN,  $[\text{CH}_3\text{--CH}_2\text{--NH}_4]^+[\text{NO}_3]^-$ ) and its hydroxyl derivative (HOEAN,  $[\text{HO--CH}_2\text{--CH}_2\text{--NH}_4]^+[\text{NO}_3]^-$ ). Besides the importance these systems may have due to the interest in extraction processes, this work allows also a theoretical characterization to be obtained of the nitrato-lanthanate(III) anions that have been seen to be one of the main complexed species that exists in the chemical

Received: July 3, 2015

Revised: August 18, 2015

Published: August 20, 2015

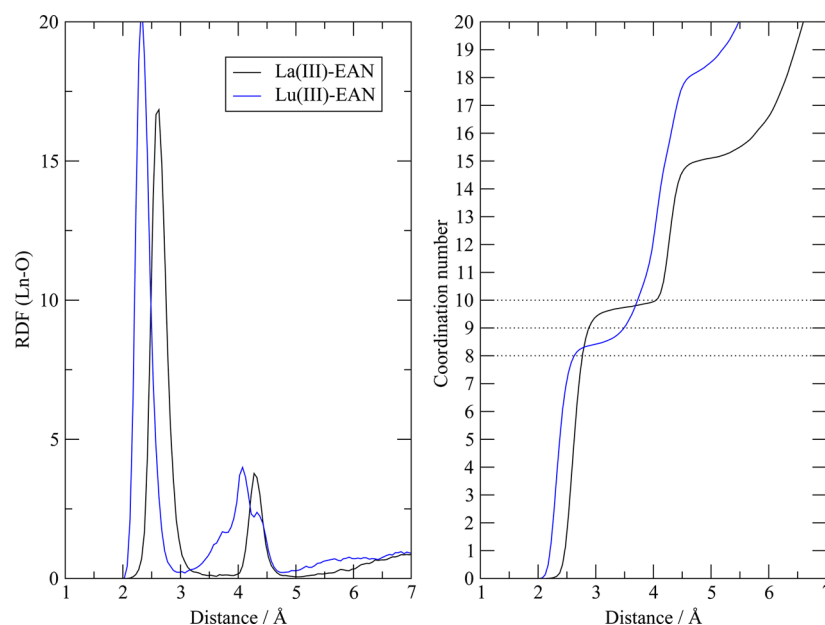


**Figure 1.** Left: RDF for the Ln(III)–O distance. Right: integral of the RDF, i.e., the coordination number of La<sup>3+</sup> with respect to O.

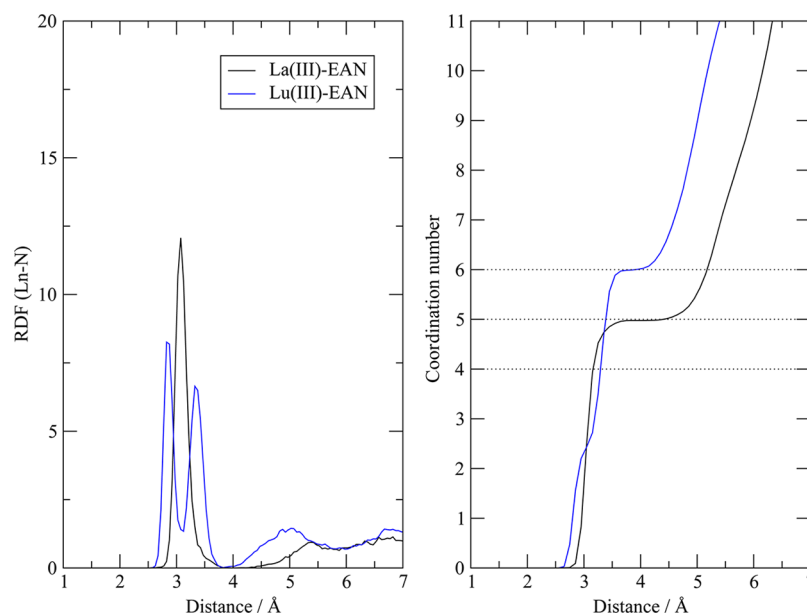


**Figure 2.** Left: RDF for the Ln(III)–N distance. Right: integral of the RDF, i.e., the coordination number of La<sup>3+</sup> with respect to N.

environment for the extraction processes using concentrated HNO<sub>3</sub>.<sup>26,27</sup> Previous studies of the nitrate complexes of lanthanoid(III) ions have mainly focused on the description of nitrate complexes in aqueous solutions or in organic solvents (see ref 28 and references therein). We provide here, for the first time, a simulation of these ions in an environment that is a pure electrolyte with no water.

## COMPUTATIONAL DETAILS

The CPMD code<sup>29</sup> has been used for the calculations. The initial liquid cells have been created by means of classical molecular dynamics employing the OPLS<sup>30</sup> force field and a suitable choice of the Ln(III) Lennard-Jones parameters (we have used the parameters reported in the standard OPLSAA force field that are  $\sigma = 3.75$  Å and  $\epsilon = 0.06$  kcal). NPT (298 K and 1 atm) classical molecular dynamics has been performed to

provide sufficiently equilibrated initial configurations that turned out to have densities of 1.21 and 1.34 g/cm<sup>3</sup> for EAN and HOEAN, respectively (these densities compare well with the experimental values reported in our previous work on the same RTILs<sup>31</sup>). The initial cells have a side length of 15.53 and 15.60 Å for EAN and HOEAN, respectively, and contain 24 ionic couples plus the Ln<sup>3+</sup> ion. Car–Parrinello molecular dynamics has been performed employing the BLYP functional and Troullier–Martins<sup>32</sup> pseudopotentials (PP) for first row elements. The La<sup>3+</sup> pseudopotential has been taken from ref 33 and that for Lu<sup>3+</sup> from ref 34. The energy cutoff on the plane waves has been set to 120 bohr and the fictitious electronic mass to 350. Starting from the classical configuration, we have performed a geometric minimization followed by an equilibration of about 6–7 ps (depending on the system) using a simple ion velocity rescaling technique for temperature control. The

production part of the MD has been propagated with a 3 au time step in the NVT ensemble (298 K) with the Nosé–Hoover thermostat for a total simulation time ranging from 30 to 60 ps depending on the systems. The deuterium atom has been used instead of hydrogen to ensure a proper propagation with the chosen time step and to reduce zero point energy inaccuracy due to the quantum nature of the bond involving hydrogen. The total propagation time is certainly sufficient to provide a relaxed shell configuration albeit not long enough to allow us to see ligand exchanges which is a process that can take place on time scales of the order of ns especially when highly cohesive liquids such as ILs are involved. Some of the postprocessing analysis has been done using the Travis program.<sup>35</sup>

The parameter selection and a test on the usability of the PP has been performed by optimizing the cell structure of the tris(1,3-dimethyl-1*H*-imidazol-3-ium) hexanitrate-lanthanum<sup>36</sup> whose crystal structure is known experimentally (CCDC Number 910702). The crystal cell of this solid contains one  $\text{La}^{3+}$  ion, three imidazole cations, and six nitrate anions that are coordinating the central charged ion. The crystallographic structure has been fed into the geometry optimization module of the CPMD code. The geometric optimization has been performed in 63 step up to a convergence of 0.001 on the total gradient. The total final RMSD deviation between the initial and final structures was very small and equal to 0.06 Å. Therefore, we expect the chosen PP to be sufficiently accurate in determining the geometrical structure of the  $\text{La}^{3+}$  ion in our simulations.

## RESULTS AND DISCUSSION

**$\text{La}^{3+}$  and  $\text{Lu}^{3+}$  in EAN.** We begin by showing the radial distribution functions of the two  $\text{Ln}^{3+}$  ions in the EAN IL in

**Table 1.** Average, Maximum, and Coordination Number of the  $\text{Ln}^{3+}$ –O and  $\text{Ln}^{3+}$ –N Distance Distributions as Obtained by Our Calculations

system	$\text{Ln}^{3+}$ –O		$\text{Ln}^{3+}$ –N	
	average (maximum)	CN	average (maximum)	CN
La@EAN	2.65 (2.60)	10	3.11 (3.07)	5
Lu@EAN	2.37 (2.32)	8.5	3.12 <sup>a</sup>	6
La@HOEAN	2.62 (2.58)	10	3.08 (3.02)	4
Lu@HOEAN	2.37 (2.32)	8	3.25 <sup>b</sup>	5

<sup>a</sup>The distribution is bimodal with two peaks (with maxima at 2.86 and 3.32 Å). <sup>b</sup>The distribution is bimodal with two peaks (with maxima at 2.87 and 3.37 Å).

**Figure 1.** The main coordinating ligand is obviously the nitrate ion, and therefore, we show the  $\text{Ln}^{3+}$ –O distance. The RDF has two clear distinct peaks owing to the fact that, once the nitrate has bound to the ion through one or two oxygen atoms (the peak around 3 Å), at least one of the other oxygen atoms remains free and points far from the ion (the smaller peak at 4 Å). As we can see from the data on the right, where we report the integral of the RDF, i.e., the coordination number (CN) of the  $\text{Ln}^{3+}$  ion, the total number of oxygen atoms coordinated up to 5 Å is 15 for  $\text{La}^{3+}$  and 18 for  $\text{Lu}^{3+}$ , therefore indicating that  $\text{La}^{3+}$  is coordinating 5 nitrate anions while the  $\text{Lu}^{3+}$  is coordinating 6. The total number of “first shell” La–O contacts is slightly below 10 for  $\text{La}^{3+}$ , while it is about 8.5 for  $\text{Lu}^{3+}$  in accord with the decreasing ionic radii along the lanthanoid series.

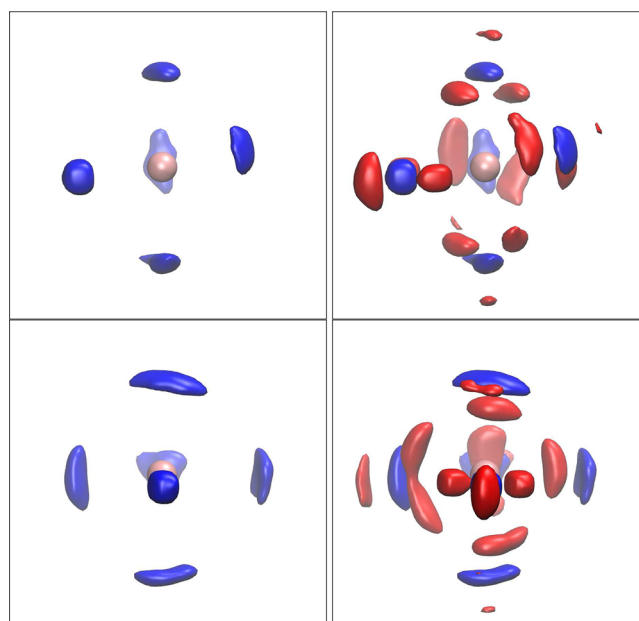


**Figure 3.** First row, left: SDF relative to N atom surrounding the  $\text{La}^{3+}$  ion. First row, right: SDF of N and O atoms around the  $\text{La}^{3+}$  ion. Second row: same as above but for the  $\text{Lu}^{3+}$  ion.

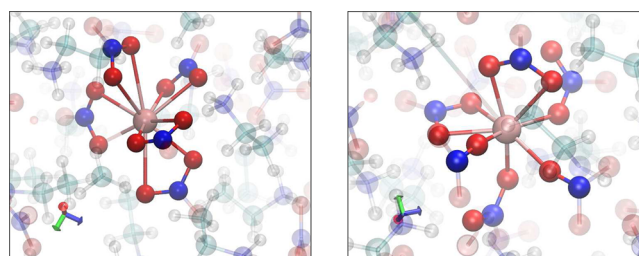


**Figure 4.** Selected snapshots of the MD trajectory: left,  $\text{La}^{3+}$ @EAN; right,  $\text{Lu}^{3+}$ @EAN. The atoms whose distances are within 4 Å from the central ion are opaque, while the rest of the system is rendered transparent. The bonds between the central ion and the oxygen atoms have been added for ease of interpretation.

In order to understand the exact geometric configuration of the ion, we report in **Figure 2**, in the same fashion as in **Figure 1**, the relevant data taken with respect to the N atom. As we can see, the number of nitrate molecules in the first shell is 5 and 6 for  $\text{La}^{3+}$  and  $\text{Lu}^{3+}$ , respectively. This means that in the case of  $\text{La}^{3+}$  all of the 5 nitrate molecules act as bidentate ligands with a total of 10 La–O well-defined contacts, while for  $\text{Lu}^{3+}$  the situation is more complex, as only about 2 or 3 of the 6 molecules seems to act as a bidentate ligand with a total oxygen CN of 8.5. The preference of  $\text{La}^{3+}$  for a bidentate complexation has been noticed before as well as the tendency of an increase of monodentate configurations in the “smaller” cations as  $\text{Lu}^{3+}$ .<sup>37</sup> This behavior is clearly shown by the asymmetry of the first solvation shell of the  $\text{Lu}^{3+}$  ion that produces two distinct peaks in the Lu–N RDF, as indicated by the data in the left panel of **Figure 2**.

In general, the RDFs of the  $\text{Ln}^{3+}$ –O distances are expected to have peaks at lower distances when moving from  $\text{La}^{3+}$  to  $\text{Lu}^{3+}$  owing to the decreasing ionic radius of the  $\text{Ln}^{3+}$  ions along the series. This decrease in the average  $\text{Ln}^{3+}$ –O distance is clearly shown by the data in the left panel of **Figure 1** where the average Ln–O distance moves from 2.65 Å in  $\text{La}^{3+}$  to 2.37 Å in

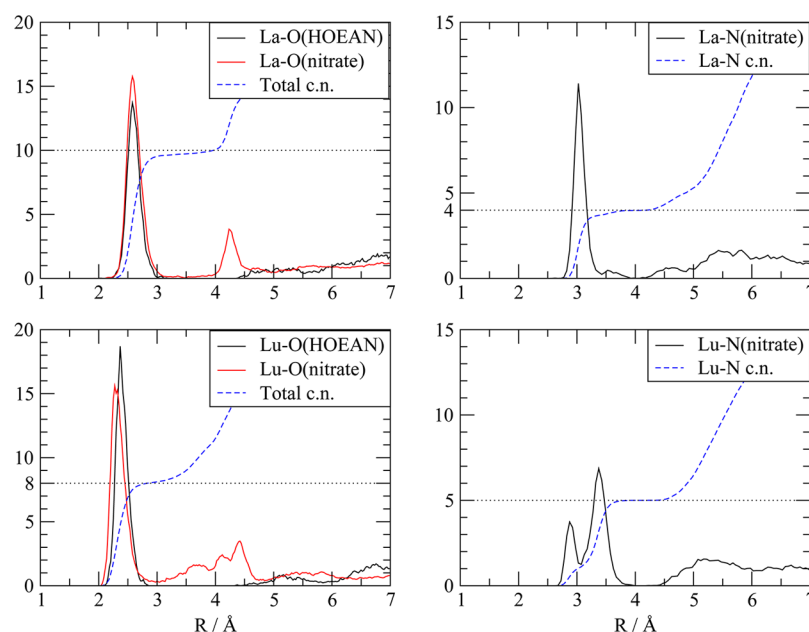


**Figure 5.** Left: RDF for the  $\text{Ln}^{3+}$ –O distance and relative coordination number. Right: RDF for the  $\text{Ln}^{3+}$ –N distance and relative coordination number.

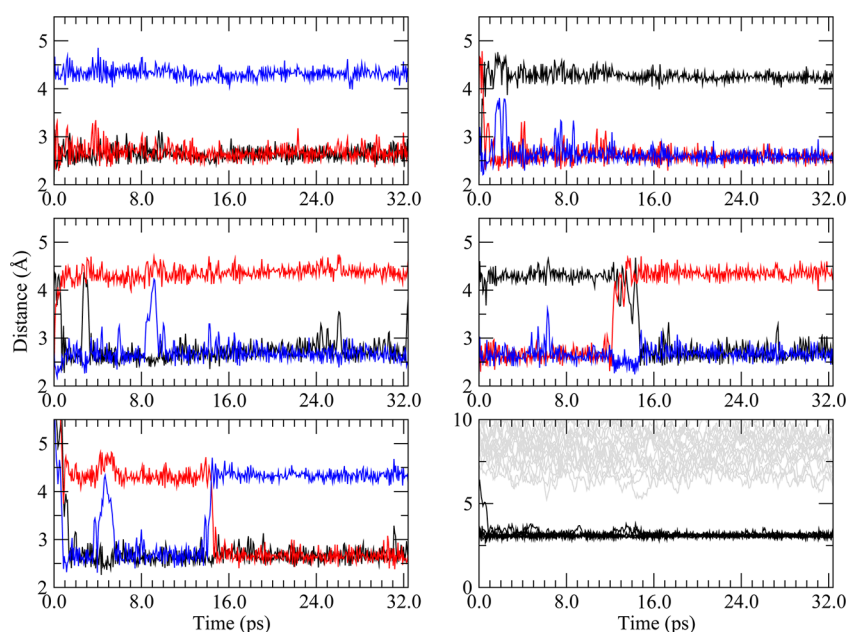


**Figure 6.** Time development for the  $\text{La}$ –O distances in each  $\text{NO}_3$  molecule bound to the  $\text{La}^{3+}$  ion. There are five nitrate molecules in the first shell, and for each of these, we report the three  $\text{La}^{3+}$ –O distances in the first five panels. The sixth panel (bottom right) shows all of the 24  $\text{La}^{3+}$ –N distances that allow the unambiguous identification of the nitrates that are near the central ion.

$\text{Lu}^{3+}$ . For other solvents such as water<sup>38</sup> or DMSO,<sup>39</sup> the decrease in ionic radius naturally leads to a corresponding decrease in the average coordination number. However, due to the bidentate nature of the nitrate ligand, here we see the opposite effect: the coordination number when we count the number of anions directly connected to the central ion is increasing along the lanthanoid(III) series despite the reduction in the average  $\text{Ln}^{3+}$ –O distance. The results are summarized in Table 1 where we report the average (weighted)  $\text{Ln}^{3+}$ –O and  $\text{Ln}^{3+}$ –N distances and the coordination numbers.

In order to elucidate this effect and therefore the innermost shell structure, we have calculated the *spatial distribution*

*function* (SDF) of the N and O atoms of the first five or six nitrate molecules by fixing the reference frame on the  $\text{Ln}^{3+}$  central ion and two oxygen atoms of one nitrate molecule. The results are reported in Figure 3 where we show the iso-surface of the spatial distributions for O and N atoms around the central ion cut so as to include roughly 5% of the total atom density.

What we get from Figure 3 is very clear geometrical information. The  $\text{La}^{3+}$  ion coordinates five nitrate anions in a slightly irregular triangular bipyramidal shape (see first row, left panel of Figure 3 where only the N atom density is reported). All 5 nitrate molecules behave as bidentate ligands with two



La–O contacts for a total coordination number of oxygen atoms in the first shell of 10. The  $\text{Lu}^{3+}$  ion, instead, coordinates 6 anions in an octahedral shape where only 3 of these act as bidentate ligands so that the oxygen coordination number in the first shell is really reduced from 10 to 8.5 accordingly to the sizable reduction of the ionic radius of  $\text{Lu}^{3+}$  with respect to  $\text{La}^{3+}$ . Therefore, what might initially appear as an inconsistency in the coordination number is really due to the more complex docking geometry of a bidentate ligand with respect to a simpler situation such as those in water and DMSO. The shell of oxygen atoms around  $\text{La}^{3+}$  does not have a clear geometric shape but due to the mobility of the ligands (see below) is rather disordered. The oxygen atoms around  $\text{Lu}^{3+}$  are also disordered, and we were unable to identify a simple geometric pattern. Two snapshots have been extracted from the simulations and are reported in Figure 4 as examples to illustrate the behavior described above.

**$\text{La}^{3+}$  and  $\text{Lu}^{3+}$  in HOEAN.** The situation that we have described in the previous section undergoes, perhaps surprisingly, a significant change when using the HOEAN solvent instead of EAN. What we see is that the oxygen atom of the cation becomes quickly incorporated into the first solvation shell substituting partially the nitrate anion. The counter-intuitive possibility of the molecular cation to solvate a positive ion is due to its size, which allows the positive charge that resides on the  $-\text{NH}_4^+$  portion of the molecule to remain far enough (more than 4 Å) from the central cation so that the residual repulsive interaction is small. The results concerning the HOEAN simulations are summarized in Figure 5 where we report the  $\text{Ln}^{3+}\text{--O}$  and  $\text{Ln}^{3+}\text{--N}$  RDFs. We can see that the radial distribution of the oxygen atoms pertaining to the HOEAN molecule is clearly part of the first solvation shell. The total coordination number of the oxygen atoms and their shape remains the same as in the EAN case: 10 for  $\text{La}^{3+}$  and 8 for  $\text{Lu}^{3+}$ . If we look on the right panel of Figure 5, we see that the coordination number of nitrogen atoms is reduced by one both for  $\text{La}^{3+}$  and for  $\text{Lu}^{3+}$  where two HOEAN molecules have entered in the first shell substituting one bidentate nitrate ligand each.

In both cases, we have also found that the coordination of HOEAN is probably promoted because of the simultaneous formation of strong hydrogen bonds between the acidic proton of the hydroxyl terminal and the oxygen atom of the nitrate anions in the first shell.

**Dynamics.** The duration of our simulations does not allow us to see much of the dynamics going on in the system. The total simulation time of 30 ps is not sufficient to explore the intershell mobility of the ligands surrounding the ions. However, it is possible to see a certain degree of dynamical motion in the first shell that takes place on short time scales. In particular, we can see that during the dynamics the relative positions of the nitrate anions change and some of them are rotating. This effect is shown in Figure 6 for the  $\text{La}^{3+}\text{@EAN}$  system where we report the distance of the inner  $\text{La}^{3+}\text{--O}$  and  $\text{La}^{3+}\text{--N}$  contacts in the first solvation shell. As we have shown above, the  $\text{La}^{3+}$  ion in our simulations is penta-coordinated with five nitrate anions. The total number of La–O contacts is 10. For each of the five nitrate molecules, we report the three possible La–O distances along 30 ps of trajectory. As is clear from the data in Figure 6, we see that there is a rapid rotation of two of the five nitrate groups at about 16 ps. This rotation is seen as an exchange of two of the distances reported in the fourth and fifth panels of Figure 6. No other exchange

processes are to be seen in the limited time span of our simulations. The results for the other systems are very similar to this one, and we do not report them.

## CONCLUSIONS

In conclusion, we have analyzed for the first time with ab initio molecular dynamics the solvation structure of  $\text{La}^{3+}$  and  $\text{Lu}^{3+}$  in two typical ionic liquids with a strong protic environment using ab initio MD. The dynamics have been carried out for a time span of 30–60 ps, and therefore, we have focused this initial effort only on the structural features of the resulting complexes. The geometry of the first solvation shell is obviously dependent on the size of the central ion, and as it is well-known,  $\text{Lu}^{3+}$  is much smaller than  $\text{La}^{3+}$  in terms of its ionic radii. We have determined that the total number of nitrate anions coordinated to the central ion in  $\text{La@EAN}$  and in  $\text{Lu@EAN}$  is 5 and 6, respectively. Despite these apparently contradictory results, we have also seen that the number of  $\text{Ln}^{3+}\text{--O}$  contacts in the first shell for the two systems is 10 for the former and 8 for the latter in accord with the decreasing ionic radii dimension of the  $\text{La}^{3+}$  ions. What happens is that while for  $\text{La}^{3+}$  the five nitrates are uniformly distributed around the central ion and all act as bidentate ligands, in the  $\text{Lu@EAN}$  case, we have an asymmetric solvation structure where only three of the nitrate ions act as a bidentate ligand while the other three are able to coordinate the central ion with only one contact each. Unexpectedly, when EAN is replaced by HOEAN, the solvation of the central ion is due to both anions and cations. We have seen that one of the nitrate anions is substituted by two ammonium cations that coordinate the central ions through their OH terminals. This peculiar process is driven by the formation of hydrogen bonds between the nitrate molecules coordinating the central ion and the OH groups on the cation.

## AUTHOR INFORMATION

### Corresponding Author

\*E-mail: [enrico.bodo@uniroma1.it](mailto:enrico.bodo@uniroma1.it).

### Notes

The authors declare no competing financial interest.

## ACKNOWLEDGMENTS

Financial support of the Scientific Committee of the University of Rome through grant “Ricerca 2014” and the computational PRACE grant N. RA1279 are gratefully acknowledged. We are grateful to R. Spezia for providing us with the PP used in the computations.

## REFERENCES

- (1) Sui, N.; Huang, K.; Zhang, C.; Wang, N.; Wang, F.; Liu, H. Light, Middle, and Heavy Rare-Earth Group Separation: A New Approach via a Liquid-Liquid-Liquid Three-Phase System. *Ind. Eng. Chem. Res.* **2013**, *52*, 5997–6008.
- (2) Radhika, S.; Kumar, B. N.; Kantam, M. L.; Reddy, B. R. Liquid-liquid Extraction and Separation Possibilities of Heavy and Light Rare-earths from Phosphoric Acid Solutions with Acidic Organophosphorus Reagents. *Sep. Purif. Technol.* **2010**, *75*, 295–302.
- (3) Banda, R.; Jeon, H.; Lee, M. Solvent Extraction Separation of Pr and Nd from Chloride Solution Containing La Using Cyanex 272 and its Mixture with Other Extractants. *Sep. Purif. Technol.* **2012**, *98*, 481–487.
- (4) Fontana, D.; Pietrelli, L. Separation of Middle Rare Earth by Solvent Extraction Using 2-ethylhexylphosphonic Acid Mono-2-ethylhexyl Ester as an Extraction. *J. Rare Earths* **2009**, *27*, 830–833.

- (5) Mudring, A.-V.; Tang, S. Ionic Liquids for Lanthanide and Actinide Chemistry. *Eur. J. Inorg. Chem.* **2010**, 2010, 2569–2581.
- (6) Cocalia, V. A.; Gutowski, K. E.; Rogers, R. D. The Coordination Chemistry of Actinides in Ionic Liquids: A Review of Experiment and Simulation. *Coord. Chem. Rev.* **2006**, 250, 755–764 (Actinide Chemistry).
- (7) Visser, A. E.; Rogers, R. D. Room-temperature Ionic Liquids: New Solvents for f-element Separations and Associated Solution Chemistry. *J. Solid State Chem.* **2003**, 171, 109–113.
- (8) Vasudeva Rao, P. R.; Venkatesan, K. A.; Rout, A.; Srinivasan, T. G.; Nagarajan, K. Potential Applications of Room Temperature Ionic Liquids for Fission Products and Actinide Separation. *Sep. Sci. Technol.* **2012**, 47, 204–222.
- (9) Mincher, B. J.; Wishart, J. F. The Radiation Chemistry of Ionic Liquids: A Review. *Solvent Extr. Ion Exch.* **2014**, 32, 563–583.
- (10) Rogers, R. D.; Seddon, K. R., Eds. *Ionic Liquids IIIA: Fundamentals, Progress, Challenges, and Opportunities: Properties and Structure*; ACS Symposium Series; American Chemical Society: Washington, DC, 2005; Vol. 901, p 356.
- (11) Gaune-Escard, M.; Seddon, K. R., Eds. *Molten Salts and Ionic Liquids: Never the Twain?*; John Wiley & Sons, Inc.: Hoboken, NJ, 2010; p 441.
- (12) Kirchner, B., Ed. *Ionic Liquids*; Topics in Current Chemistry; Springer: Berlin Heidelberg, 2012; Vol. 290.
- (13) Caminiti, R.; Gontrani, L., Eds. *The structure of Ionic Liquids*; Soft and Biological Matter; Springer International Publishing: Switzerland, 2014; Vol. 193.
- (14) Greaves, T. L.; Drummond, C. J. Protic Ionic Liquids: Properties and Applications. *Chem. Rev.* **2008**, 108, 206–237.
- (15) Fumino, K.; Peppel, T.; Geppert-Rybczynska, M.; Zaitsau, D. H.; Lehmann, J. K.; Verevkin, S. P.; Köckerling, M.; Ludwig, R. The influence of hydrogen bonding on the physical properties of ionic liquids. *Phys. Chem. Chem. Phys.* **2011**, 13, 14064–14075.
- (16) Zahn, S.; Thar, J.; Kirchner, B. Structure and Dynamics of the Protic Ionic Liquid Monomethylammonium Nitrate from Ab Initio Molecular Dynamics Simulations. *J. Chem. Phys.* **2010**, 132, 124506.
- (17) Bodo, E.; Sferrazza, A.; Caminiti, R.; Mangialardo, S.; Postorino, P. A Prototypical Ionic Liquid Explored by Ab Initio Molecular Dynamics and Raman Spectroscopy. *J. Chem. Phys.* **2013**, 139, 144309.
- (18) Bodo, E.; Mangialardo, S.; Capitani, F.; Gontrani, L.; Leonelli, F.; Postorino, P. Interaction of a Long Alkyl Chain Protic Ionic Liquid and Water. *J. Chem. Phys.* **2014**, 140, 204503.
- (19) Maginn, E. J. Molecular Simulations of Ionic Liquids: Current Status and Future Opportunities. *J. Phys.: Condens. Matter* **2009**, 21, 373101.
- (20) Del Popolo, M. G.; Lynden-Bell, R. M.; Kohanoff, J. Ab Initio Molecular Dynamics Simulation of a Room Temperature Ionic Liquid. *J. Phys. Chem. B* **2005**, 109, 5895–5902.
- (21) Schmidt, J.; Krekeler, C.; Dommert, F.; Zhao, Y.; Berger, R.; Site, L. D.; Holm, C. Ionic Charge Reduction and Atomic Partial Charges from First-Principles Calculations of 1,3-Dimethylimidazolium Chloride. *J. Phys. Chem. B* **2010**, 114, 6150–6155.
- (22) Wendler, K.; Zahn, S.; Dommert, F.; Berger, R.; Holm, C.; Kirchner, B.; Delle Site, L. Locality and Fluctuations: Trends in Imidazolium-Based Ionic Liquids and Beyond. *J. Chem. Theory Comput.* **2011**, 7, 3040–3044.
- (23) Zahn, S.; Wendler, K.; Delle Site, L.; Kirchner, B. Depolarization of water in protic ionic liquids. *Phys. Chem. Chem. Phys.* **2011**, 13, 15083–15093.
- (24) Dommert, F.; Schmidt, J.; Krekeler, C.; Zhao, Y. Y.; Berger, R.; Site, L. D.; Holm, C. Towards Multiscale Modeling of Ionic Liquids: From Electronic Structure to Bulk Properties. *J. Mol. Liq.* **2010**, 152, 2–8.
- (25) Izgorodina, E. I. Towards Large-scale Fully Ab Initio Calculations of Ionic Liquids. *Phys. Chem. Chem. Phys.* **2011**, 13, 4189–4207.
- (26) Eriksson, B.; Larsson, L. O.; Niinistö, L.; Valkonen, J. Crystal and Molecular Structure of the Undecacoordinate Complex Pentaquatrakis(Nitrato)Lanthanum(III) Monohydrate. *Inorg. Chem.* **1980**, 19, 1207–1210.
- (27) Ji, S.-P.; Tang, M.; He, L.; Tao, G.-H. Water-Free Rare-Earth-Metal Ionic Liquids/Ionic Liquid Crystals Based on Hexanitratolanthanate(III) Anion. *Chem. - Eur. J.* **2013**, 19, 4452–4461.
- (28) Duvail, M.; Guilbaud, P. Understanding the Nitrate Coordination to Eu<sup>3+</sup> Ions in Solution by Potential of Mean Force Calculations. *Phys. Chem. Chem. Phys.* **2011**, 13, 5840–5847.
- (29) Hutter, J.; Alavi, A.; Deutsch, T.; Bernasconi, M.; Goedecker, D.; Marx, D.; Tuckerman, M.; Parrinello, M. CPMD, version 3.9.1; IBM Research Division, IBM Corp and Max Planck Institute Stuttgart: 2004.
- (30) Jorgensen, W. L.; Maxwell, D. S.; Tirado-Rives, J. Development and Testing of the OPLS All-Atom Force Field on Conformational Energetics and Properties of Organic Liquids. *J. Am. Chem. Soc.* **1996**, 118, 11225–11236.
- (31) Gontrani, L.; Bodo, E.; Triolo, A.; Leonelli, F.; D'angelo, P.; Migliorati, V.; Caminiti, R. The Interpretation of Diffraction Patterns of Two Prototypical Protic Ionic Liquids: a Challenging Task for Classical Molecular Dynamics Simulations. *J. Phys. Chem. B* **2012**, 116, 13024–13032.
- (32) Troullier, N.; Martins, J. L. Efficient Pseudopotentials for Plane-Wave Calculations. *Phys. Rev. B: Condens. Matter Mater. Phys.* **1991**, 43, 1993.
- (33) Terrier, C.; Vitorge, P.; Gaigeot, M.-P.; Spezia, R.; Vuilleumier, R. Density Functional Theory Based Molecular Dynamics Study of Hydration and Electronic Properties of Aqueous La<sup>3+</sup>. *J. Chem. Phys.* **2010**, 133, 044509.
- (34) Martelli, F.; Jeanvoine, Y.; Vercouter, T.; Beuchat, C.; Vuilleumier, R.; Spezia, R. Hydration properties of Lanthanoid(III) Carbonates Complexes in Liquid Water by Polarizable Molecular Dynamics Simulations. *Phys. Chem. Chem. Phys.* **2014**, 16, 3693–3705.
- (35) Brehm, M.; Kirchner, B. TRAVIS - A Free Analyzer and Visualizer for Monte Carlo and Molecular Dynamics Trajectories. *J. Chem. Inf. Model.* **2011**, 51, 2007–2023.
- (36) Ji, S.-P.; Tang, M.; He, L.; Tao, G.-H. Water-Free Rare-Earth-Metal Ionic Liquids/Ionic Liquid Crystals Based on Hexanitratolanthanate(III) Anion. *Chem. - Eur. J.* **2013**, 19, 4452–4461.
- (37) Dobler, M.; Guilbaud, P.; Dedieu, A.; Wipff, G. Interaction of Trivalent Lanthanide Cations with Nitrate Anions: a Quantum Chemical Investigation of Monodentate/Bidentate Binding Modes. *New J. Chem.* **2001**, 25, 1458–1465.
- (38) Duvail, M.; Spezia, R.; Vitorge, P. A Dynamical Model to explain Hydration Behaviour through Lanthanide Series. *ChemPhysChem* **2008**, 9, 693–696.
- (39) D'Angelo, P.; Migliorati, V.; Spezia, R.; De Panfilis, S.; Persson, I.; Zitolo, A. K-edge XANES Investigation of Octakis (DMSO) Lanthanoid(III) Complexes in DMSO Solution and Solid Iodides. *Phys. Chem. Chem. Phys.* **2013**, 15, 8684–8691.